



# Tunneling spectroscopy of topological superconductors



Satoshi Kashiwaya<sup>a,\*</sup>, Hiromi Kashiwaya<sup>a</sup>, Kohta Saitoh<sup>a</sup>, Yasunori Mawatari<sup>a</sup>,  
Yukio Tanaka<sup>b</sup>

<sup>a</sup> National Institute of Advanced Industrial Science and Technology (AIST), Tsukuba 305-8568, Japan

<sup>b</sup> Department of Applied Physics, Nagoya University, Nagoya 464-8603, Japan

## ARTICLE INFO

### Article history:

Received 29 May 2013

Accepted 22 July 2013

Available online 2 August 2013

### Keywords:

Tunneling spectroscopy

Andreev bound states

Topological superconductors

Gapless edge states

## ABSTRACT

Tunneling conductance spectra of normal metal/insulator/superconductor (*N/I/S*) junctions are calculated to determine the potential of tunneling spectroscopy in investigations of topological superconductivity. Peculiar feature of topological superconductors is the formation of gapless edge states in them. Since the conductance of *N/I/S* junctions is sensitive to the formation of these edge states, topological superconductivity can be identified through edge-state detection. Herein, the effects of Fermi surface anisotropy and an applied magnetic field on the conductance spectra are analyzed to gather indications that can help to identify the topological nature of actual materials.

© 2013 Elsevier B.V. All rights reserved.

## 1. Introduction

Tunneling spectroscopy has been accepted as one of the highest energy resolution probes for electronic states. Various novel phenomena relevant to superconductivity have been revealed by tunneling spectroscopy of normal metal/insulator/superconductor (*N/I/S*) junctions. Recently, there is an increasing interest in the properties of topological superconductors (TSCs), whose superconducting gap function in momentum space is topologically non-trivial [1–6]. Although novel properties of the TSCs, such as Majorana fermions at the edges and the vortex cores, have been predicted in a number of theories [7–15], the focus of most experiments remains at the level of exploring the existence of TSCs. The identification of the TSCs based on conventional experimental probes is difficult because the bulk densities of states (DOS) of most of the TSCs are similar to those of conventional superconductors. On the other hand, a peculiar feature of topological materials, the so-called “bulk-edge correspondence,” is known to induce gapless edge states formed at the edges and defects at which the translational symmetry is broken [16–18]. Therefore, the detection of these gapless states inside the superconducting gap is the manifestation of topological superconductivity in real materials.

On the other hand, unconventional superconductivity is characterized by the anisotropic gap function, whose amplitude and phase depend on the wave vector. This anisotropic gap function is known to induce Andreev bound states (ABSs) at the surfaces and interfaces where the effective pair potential for the quasiparticles

changes through reflection. The formation of ABSs has been predicted for the surface states of <sup>3</sup>He [19,20] and described for the surface states of  $d_{x^2-y^2}$ -wave superconductors [21–27]. Recently the zero-energy ABS has been reinterpreted as a topological edge state [18,28–32]; therefore, the high sensitivity of tunneling spectroscopy to surface states can make a significant contribution to our understanding of TSCs based on the observation of the edge states. Experimentally, the existence of the ABS has already been verified by the zero-bias peaks observed in the conductance spectra of *N/I/S* junctions of various high- $T_c$  cuprates [22,25]. Furthermore, the realization of the topological superconductivity and superfluidity has been suggested for Sr<sub>2</sub>RuO<sub>4</sub>, Cu-doped Bi<sub>2</sub>Se<sub>3</sub>, PdBi, and <sup>3</sup>He [33–36].

Here, we systematically analyze the conductance spectra of TSCs with various types of gap functions by comparing them with those of non-topological superconductors. We also examine the correspondence between topological superconductivity and the conductance peak shape with taking account of the sensitivity to the orientation of the tunneling junction and the effects of anisotropy. Furthermore, we discuss how to detect broken time-reversal symmetry (TRS) based on the magnetic field response of *N/I/S*.

## 2. Conductance spectra of TSCs

Herein, we consider an *N/I/S* junction with a flat interface perpendicular to the *x*-axis, as shown in Fig. 1(a). Although the superconductor is assumed to be quasi-two-dimensional with an isotropic Fermi surface in the *x*-*y* plane, for simplicity, all the results can be directly extended to the three-dimensional case.

\* Corresponding author. Tel.: +81 298615568.

E-mail address: [s.kashiwaya@aist.go.jp](mailto:s.kashiwaya@aist.go.jp) (S. Kashiwaya).

Two-dimensionality has an advantage in that the ABSs do not appear on the  $z$ -plane, so the bulk DOS can be probed using a  $z$ -axis tunneling junction without the influence of the edge states [33].

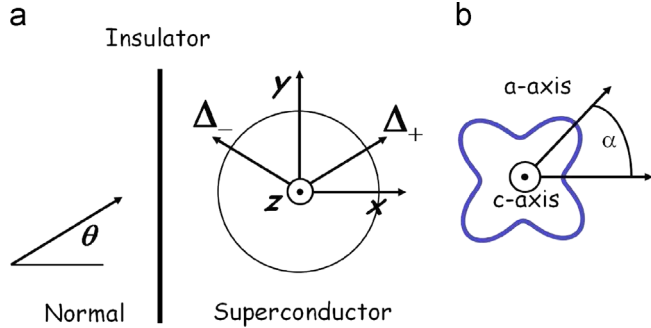


**Fig. 1.** (a) Schematic of a normal metal/insulator/superconductor junction and the quasiparticle injection from the normal metal. (b) Schematic of an anisotropy of the gap amplitude.

The gap function of the spin-singlet superconductor is represented by  $\Delta(\mathbf{k})$ , where  $\mathbf{k}$  is the wave vector of the quasiparticle in the  $xy$ -plane, and of the triplet  $\Delta_{\mathbf{k}} = [\mathbf{d}_{\mathbf{k}}, \sigma]i\sigma_y$ , where  $\sigma$  and  $\mathbf{d}_{\mathbf{k}}$  are Pauli matrices and the  $\mathbf{d}$ -vector, respectively. The angle-resolved conductance spectrum  $\sigma(\theta, eV)$  for the quasiparticle injected from the left, with the incident angle  $\theta$  and energy  $eV$  to the interface, is calculated through the extension of the BTK model [37]. The total conductance  $\sigma(eV)$  is given by integrating over all injection angles. Details of the formulation for singlet cases are described in Refs. [23,25] and for triplet cases in Refs. [18,38–41]. The conductance for a given  $\theta$  contains two distinct gap functions  $\Delta_+$  and  $\Delta_-$ , which correspond to the effective pair potentials for the transmitted electron-like and hole-like quasiparticles, respectively. The barrier potential of the insulator and the barrier parameter  $Z$  are represented by  $H\delta(x)$  and  $Z = mH/(\hbar^2 k_F)$ , respectively, where  $m$ ,  $H$ , and  $k_F$  are the electron mass, amplitude of the barrier potential, and Fermi wavelength, respectively.

We consider eight types of pairing symmetries, as listed in Table 1, by mainly taking into account of the possible candidates for  $\text{Sr}_2\text{RuO}_4$ . Fig. 2 show the calculated conductance spectra  $\sigma(\theta, eV)$  for

**Table 1**  
Eight pairing symmetries and their gap functions, spin states, time reversal symmetry (TRS), and topological invariants used in the present calculation are summarized.  $L_z$  is orbital angular momentum of a Cooper pair, and 1D means one-dimensional.

| Symmetry              | Spin    | Gap function                              | TRS | Topological invariant    |
|-----------------------|---------|---|-----|--------------------------|
| s                     | Singlet | $\Delta_0$                                | ○   | ×                        |
| $d_{x^2-y^2}$         | Singlet | $\Delta_0(k_x^2 - k_y^2)$                 | ○   | ×                        |
| $d_{xy}$              | Singlet | $\Delta_0(2k_x k_y)$                      | ○   | ID winding number[30,43] |
| $d_{xy}+is$           | Singlet | $\Delta_0(2k_x k_y) + i\Delta_s$          | ×   | ×                        |
| chiral-d              | Singlet | $\Delta_0(k_x^2 - k_y^2 + 2ik_x k_y)$     | ×   | $Z[6]$                   |
| chiral-p ( $L_z=1$ )  | Triplet | $\Delta_0(k_x + ik_y)\mathbf{z}$          | ×   | $Z[6,42]$                |
| chiral-p ( $L_z=-1$ ) | Triplet | $\Delta_0(k_x - ik_y)\mathbf{z}$          | ×   | $Z[6,42]$                |
| helical-p             | Triplet | $\Delta_0(k_y\mathbf{x} + k_x\mathbf{y})$ | ○   | $Z_2[6,40]$              |

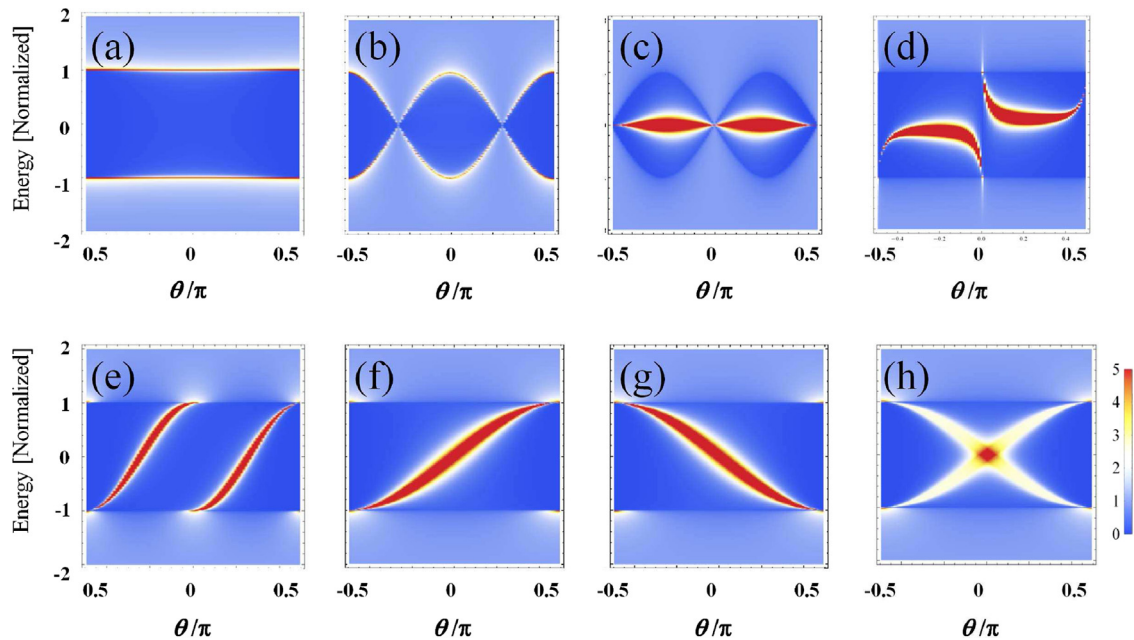


**Fig. 2.** Angle resolved conductance spectra for the eight pairing symmetries with the barrier parameter  $Z=4$ , (a) s-wave, (b)  $d_{x^2-y^2}$ -wave, (c)  $d_{xy}$ -wave, (d)  $d_{xy}+is$ -wave, (e) chiral d-wave, (f) chiral p-wave ( $L_z=1$ ), (g) chiral p-wave ( $L_z=-1$ ), and (h) helical p-wave. The color represents the magnitude of conductance of the junction, the vertical axis is the quasiparticle energy normalized by  $\Delta_0$ , and the horizontal axis is the injection angle  $\theta$ . Since the horizontal axis can be converted to a wave vector  $k_y (= k_F \sin \theta)$ , we can easily recognize the dispersion of the ABS from these figures. Red regions inside the gap correspond to the conductance peak originating from the ABS formed at the edge. When the ABS sits on the zero-energy level at a certain angle, the superconductor becomes topologically non-trivial. The amplitude of  $\Delta_s$  is assumed to be  $0.2 \Delta_0$ .

Download English Version:

<https://daneshyari.com/en/article/1544729>

Download Persian Version:

<https://daneshyari.com/article/1544729>

[Daneshyari.com](https://daneshyari.com)